

Different dynamics of classical and quantum correlations under decoherence

**Peng Huang, Jun Zhu, Xiao-xiao Qi,
Guang-qiang He & Gui-hua Zeng**

Quantum Information Processing

ISSN 1570-0755

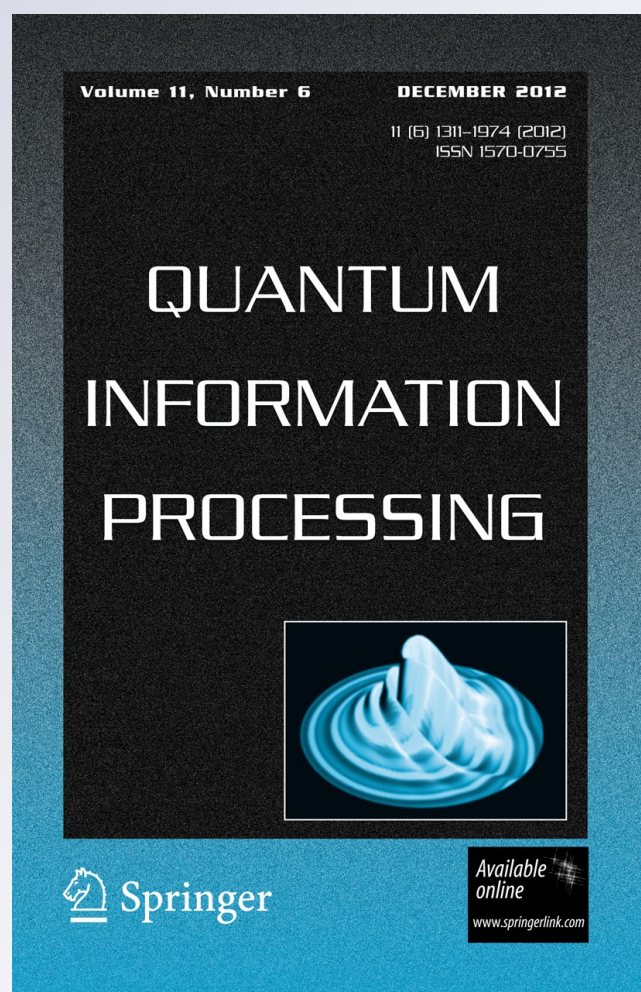
Volume 11

Number 6

Quantum Inf Process (2012)

11:1845-1865

DOI 10.1007/s11128-011-0335-x



Your article is protected by copyright and all rights are held exclusively by Springer Science+Business Media, LLC. This e-offprint is for personal use only and shall not be self-archived in electronic repositories. If you wish to self-archive your work, please use the accepted author's version for posting to your own website or your institution's repository. You may further deposit the accepted author's version on a funder's repository at a funder's request, provided it is not made publicly available until 12 months after publication.

Different dynamics of classical and quantum correlations under decoherence

Peng Huang · Jun Zhu · Xiao-xiao Qi ·
Guang-qiang He · Gui-hua Zeng

Received: 9 July 2011 / Accepted: 17 November 2011 / Published online: 1 December 2011
© Springer Science+Business Media, LLC 2011

Abstract The dynamics of classical and quantum correlations under nondissipative and dissipative decoherences are analytically and numerically investigated with both one-side measures and two-side measures. Specifically, two qubits under local amplitude damping decoherence and depolarizing decoherence channels are considered. We show that, under the action of amplitude damping decoherence, both the entanglement and correlations of the different types of initial states with same initial values, suffer different types of dynamics. Moreover, the transfers of the entanglement and correlations between the system and the environment for different types of initial states are also shown to be different. While for the action of depolarizing decoherence, there does not exist sudden change in the decay rates of both the classical and quantum correlations, which is different from some other nondissipative channels. Furthermore, the quantum dissonance can be found to keep unchanged under the action of depolarizing decoherence. Such different dynamic behaviors of different noisy quantum decoherence channels reveal distinct transmission performance of classical and quantum information.

Keywords Quantum information · Classical correlation · Quantum correlation · Decoherence channel

1 Introduction

Quantum entanglement, which reals distinctive quantum property of correlations in quantum systems, plays an essential role in understanding the nonlocality of

P. Huang (✉) · J. Zhu · X. Qi · G. He · G. Zeng
Department of Electronic Engineering, State Key Laboratory of Advanced Optical Communication Systems and Networks, Shanghai Jiaotong University, Shanghai 200240, China
e-mail: peakeagle1985@hotmail.com

quantum mechanics [1]. The entangled states can not be prepared with the help of local operation and classical communication (LOCC) [2]. Entanglement may disappear due to the interaction of a quantum system with its environment, which is known as entanglement sudden death [3,4]. However, there exist quantum effects that display the quantum feature without entanglement [5–8], such as the nonclassical features of separable states [9,10], which can be prepared using only LOCC [11]. As shown in [7,8], for the separable states which have zero entanglement but nonzero discord, the alive quantum coherence can give a speedup in performing some tasks over the best known classical counterpart in the non-universal model of quantum computation. Therefore, quantum correlations are more general and more fundamental to quantifying the quantumness of correlations. Many measures of quantum correlations have been proposed [9,12–19], and the quantum discord [9,12] has recently received a great deal of attention [7,8,20–33].

In quantum information theory, it is widely accepted that total correlations in a bipartite quantum system ρ_{AB} [17,32,34] are measured by quantum mutual information $\mathcal{I}(\rho_{AB})$ defined as

$$\mathcal{I}(\rho_{AB}) = S(\rho_A) + S(\rho_B) - S(\rho_{AB}), \quad (1)$$

where ρ_A and ρ_B are the reduced-density matrices of ρ_{AB} , and $S(\rho_{AB}) = -\text{Tr}(\rho \log_2 \rho)$ is the von Neumann entropy. It is quite nature to assume that the total correlations contained in a bipartite quantum system may be separated to quantum correlations $\mathcal{Q}(\rho_{AB})$ and classical correlations $\mathcal{C}(\rho_{AB})$, which leads to

$$\mathcal{Q}(\rho_{AB}) = \mathcal{I}(\rho_{AB}) - \mathcal{C}(\rho_{AB}). \quad (2)$$

When the classical correlations $\mathcal{C}(\rho_{AB})$ is quantified via the one-side measurement on the bipartite system [9], the quantum correlations $\mathcal{Q}(\rho_{AB})$ is just identical to quantum discord $\mathcal{D}(\rho_{AB})$. Such quantum correlation is more general than entanglement, which can be further separated as entanglement and the additional non-entanglement quantum correlation [35]. To measure the non-entanglement correlation that may be present in separable states [19], a new quantum correlation, i.e., quantum dissonance is proposed. And it has been demonstrated theoretically [7] and experimentally [8] that the separable mixed states have nonclassical correlations which leads to nonzero discord. Moreover, these nonclassical correlations can be used to perform quantum computation tasks and may have a significant role in quantum information protocols.

Understanding the dynamics of classical and quantum correlations have attracted great attention, since the interaction between the quantum system and its environment is unavoidable. It is shown that the dynamics of quantum correlations measured by quantum discord and entanglement under both Markovian [24] and Non-Markovian [26,27] environments are very different. For the Markovian evolution [24], the quantum discord decay exponentially and vanish asymptotically in the decoherence behavior, and entanglement may exhibit sudden death [3]. Recently, the studies reveal that the classical correlation may be unaffected by nondissipative decoherence [28] and the bipartite quantum correlation might completely lost without being transferred to the environment [29] for the Markovian case. Furthermore, quantum discord is

found to be also undestroyed by the nondissipative decoherence and there exists a sudden transition from classical to quantum decoherence regime [36].

In this study, we investigate the dynamics of classical and quantum correlations under two different decoherences, i.e., local nondissipative and dissipative decoherences. Specifically, we focus on two open noisy quantum channels, i.e., amplitude damping decoherence and depolarizing decoherence channel. We investigate the dynamics of classical and quantum correlations under the action of amplitude damping decoherence channel with both one-side and two-side measures, and demonstrate that the two-side measures of correlation is optimal. For different classes of initial states, the correlations are found to suffer different types of dynamics. Moreover, the transfers of correlations for different types of initial state between the bipartite quantum system and the independent environments are analyzed. On the other hand, we show analytically and numerically that sudden changes of the decay rates of both classical and quantum correlations under the action of depolarizing decoherence do not exist. Hence, neither the classical nor the quantum correlation will be unaffected by the depolarizing decoherence. However, we find the quantum dissonance, which is another measure of quantum correlation similar with quantum discord but excluding entanglement, can keep unchanged. To explore the physical origin of the different dynamic behaviors, we adopt the definition of distance measure of correlations proposed in Ref. [19].

This paper is organized as follows. In Sect. 2, we take a brief introduction about the measures of correlations, including classical correlation, quantum discord and total correlation. In Sect. 3, we investigate the dynamics of correlations under the action of amplitude damping and depolarizing decoherence, and explore the physical origin of the dynamic behaviors. Finally, the conclusions are drawn in Sect. 4.

2 Measures of correlations

2.1 Classical and quantum correlations

In classical information theory, the mutual information between two random variables A and B is given by Ref. [37]

$$I(A : B) = H(A) + H(B) - H(A, B), \tag{3}$$

where $H(X) = -\sum_x p_x \log_2 p_x$ and $H(A, B) = -\sum_{a,b} p_{a,b} \log_2 p_{a,b}$ are the Shannon entropies for $X = A, B$ and the joint system AB , respectively. $p_{a,b}$ and $p_a = \sum_b p_{a,b}$ ($p_b = \sum_a p_{a,b}$) are the joint probabilities of the variables A, B and marginal probability of $A(B)$ respectively, when the variables A and B assuming the values a and b . Also, the mutual information can be expressed in terms of the conditional entropy equivalently as

$$J(A : B) = H(A) - H(A|B), \tag{4}$$

where $H(A|B) = -\sum_{a,b} p_{a,b} \log_2 p_{a|b}$ is the conditional entropy of the variable A given the variable B . It can be seen that Eq. (1) is just the extension of Eq. (3) to a bipartite quantum state ρ_{AB} in quantum information theory. For a bipartite quantum

system ρ_{AB} , it is known that the outcome of the state of A depends on the measurement on B . Here the measurement performed on B is considered of von Neumann type and can be described by a complete set of orthonormal projector $\{\Pi_i^B\}$ on subsystem B with the outcome i . Hence, we get the quantum version of Eq. (4) as

$$\mathcal{J}(\rho_{AB}) = S(\rho_A) - S_{\{\Pi_i^B\}}(\rho_{A|B}), \tag{5}$$

where $S_{\{\Pi_i^B\}}(\rho_{A|B}) = \sum_i q_i S(\rho_A^i)$ is the conditional entropy of subsystem A , given the knowledge of the state of B , with $\rho_A^i = \text{Tr}_B((\mathbb{I}_A \otimes \{\Pi_i^B\})\rho_{AB}(\mathbb{I}_A \otimes \{\Pi_i^B\})) / p_i$ and $p_i = \text{Tr}_{AB}[(\mathbb{I}_A \otimes \{\Pi_i^B\})\rho_{AB}]$, \mathbb{I}_A is the identity operator on subsystem A .

For bipartite quantum states, one-side classical correlation between two subsystems can be quantified as Ref. [9]

$$\mathcal{C}(\rho_{AB}) = \max_{\{\Pi_i^B\}} [S(\rho_A) - S_{\{\Pi_i^B\}}(\rho_{A|B})], \tag{6}$$

where the maximum is taken over the complete set of projective measurements $\{\Pi_i^B\}$ on subsystem B , since projective measurement is demonstrated to be the optimal measurement rather than the other general positive operator-valued measurements for bipartite system. Different from the classical information theory, the Eqs. (1) and (6) are not equivalent for correlated bipartite quantum states, the difference is just the quantum discord $\mathcal{D}(\rho_{AB})$.

Two-side measures of correlations, which are proposed in Refs. [13–15, 29], is the extension of one-side measures of correlations. The two-side classical correlation, which can be calculated by local measurements on both subsystems of the bipartite state, can be expressed as the ‘‘maximum classical mutual information’’ as

$$\mathcal{C}_l(\rho_{AB}) = \max_{\{\Pi_i^A \otimes \Pi_j^B\}} I(\rho_{AB}), \tag{7}$$

where $I(\rho_{AB})$ is the classical mutual information defined in Eq. (3), in which $H(A)$, $H(B)$, and $H(A, B)$ are the entropies of the probability distribution of subsystems A and B and the composite system AB while performing a set of local projective measurements $\{\Pi_i^A \otimes \Pi_j^B\}$ on both subsystems. Thus, the two-side measures of quantum correlation is given by

$$\mathcal{Q}_l(\rho_{AB}) = \mathcal{I}(\rho_{AB}) - \mathcal{C}_l(\rho_{AB}). \tag{8}$$

It is worth noting that whether the one-side or the two-side measure, the classical correlation naturally corresponds to the maximum classical mutual information that can be obtained by local measurements on the composite system AB . The difference is the type of the local measurements which are used to evaluate the classical correlation. In some cases, the maximum classical mutual information obtained by the two-side measurement will be larger than the one-side measurement. Hence, the two-side measure of classical correlation may be more suitable in these cases. In the following, we will show that the two-side measure of classical correlation is more precise than the one-side one when considering the dynamics of correlations under amplitude damping

decoherence. However, for the bipartite states with maximally mixed marginal, the two-side measures of classical and quantum correlations are numerically verified the same as the the one-side measures of the corresponding correlations [29].

2.2 Relative entropy as a distance measure of correlations

To unify different measures of quantum correlations and make the known notions including entanglement, quantum discord, classical correlation and total correlation coincide with each others, the concept of relative entropy as a measure distance is used to classify the different correlations in Ref. [19].

When the distance is measured by relative entropy, for a given composite quantum state, the distance to its closest separable state is the measure of relative entropy of entanglement [38,39]. Also, the distance to its closest classical state is the measure of quantum discord \mathcal{D} , and this closest classical state to the closest product state of the closest classical state is the measure of classical correlation \mathcal{C} [19]. Furthermore, a new quantum correlation, quantum dissonance \mathcal{Q}_d , is defined as the distance from the closest separable state of the given state to the closest classical state of the separable state. The dissonance is a measure of nonclassical correlation excluding entanglement. For the Bell-diagonal state ρ_{AB} , the quantum dissonance \mathcal{Q}_d is given by

$$\mathcal{Q}_d(\rho_{AB}) = 1 + \sum_{i=1}^4 p_i \log_2 p_i - (p_1 + p_2) \log_2(p_1 + p_2) - (1 - p_1 - p_2) \log_2(1 - p_1 - p_2), \tag{9}$$

where $p_1 = 1/2$, $p_i = \lambda_i/2(1 - \lambda_1)$, and $\lambda_1 \geq \lambda_2 \geq \lambda_3 \geq \lambda_4$ are the four eigenvalues of state ρ_{AB} .

3 Dynamics of correlations under decoherence

In this section, we will investigate the dynamics of the classical and quantum correlations as well as the entanglement under the action of two different types of noisy channels, i.e., the dissipative and nondissipative quantum channels. Especially, we focus on two exact channels, i.e., the amplitude damping channel and depolarizing channel.

Our main goal here is to investigate the dynamics of classical and quantum correlations as well as entanglement under noisy decoherence channels for different types of initial states. In this study, we consider the scenario of two qubits under decoherence channels, where the two qubits are a class of general two-qubit states with maximally mixed marginals in the form

$$\rho_{AB} = \frac{1}{4} \left(I_{AB} + \sum_{i=1}^3 c_i \sigma_i^A \otimes \sigma_i^B \right), \tag{10}$$

where σ_i^k is the standard Pauli matrix in direction i acting on the subspace $k = A, B$, and c_i are real coefficients such that $0 \leq |c_i| \leq 1$ for $i = 1, 2, 3$. This class of states include the Werner states ($|c_1| = |c_2| = |c_3| = c$) and Bell states ($|c_1| = |c_2| = |c_3| = 1$).

Mathematically, a quantum channel can be represented by a completely positive, trace-preserving (CPTP) linear map \mathcal{N} , which maps from $\mathcal{B}(\mathcal{H}_1)$ to $\mathcal{B}(\mathcal{H}_2)$, where $\mathcal{B}(\mathcal{H})$ denotes the set of bounded linear operators on the space \mathcal{H} , \mathcal{H}_1 and \mathcal{H}_2 are the input and output Hilbert space. According to the Kraus representation theorem [40], the evolution of two-qubits state ρ_{AB} under the multimode quantum channel can be expressed as

$$\mathcal{N}(\rho_{AB}) = \sum_{i,j} (\Gamma_i^A \otimes \mathbf{I}_B)(\mathbf{I}_A \otimes \Gamma_j^B)\rho_{AB}(\mathbf{I}_A \otimes \Gamma_j^B)^\dagger (\Gamma_i^A \otimes \mathbf{I}_B)^\dagger, \tag{11}$$

where Γ_i^k ($k = A, B$) are the Kraus operators that describe the noise channels performing on subsystem k .

3.1 Amplitude damping channel

We first consider the dynamics of correlations under amplitude damping decoherence with initial state ρ_{AB} given by Eq. (10). The amplitude damping channel \mathcal{N}_A exhibits dissipative interaction between the quantum system and the environment, since there is an exchange of energy between the system and the environment. The Kraus operators are given by Ref. [41]

$$\Gamma_0^k = \begin{pmatrix} 1 & 0 \\ 0 & \sqrt{1-p_k} \end{pmatrix}, \Gamma_1^k = \begin{pmatrix} 0 & \sqrt{p_k} \\ 0 & 0 \end{pmatrix}, \tag{12}$$

with $k = A, B$. It should be mentioned that we use the general parameterized time $p_k \in [0, 1]$ to describe the dynamical evolution of the system under the action of decoherence channels, since it accounts for a large range of physical scenarios. For instance, considering an infinite bosonic environment interacting with a two-level fermionic system under Markovian approximation, p_k will be a decreasing exponential function of time [29]. We consider here the symmetric situation in which the decoherence rates of both channels are equal, i.e., $p_A = p_B \equiv p$.

The density operator of the output state $\mathcal{N}_a(\rho_{AB})$ under the multimode amplitude damping channel is given by

$$\rho_{AB}^a(p) = \frac{1}{4} \begin{pmatrix} c_3q^2 + (1+p)^2 & 0 & (c_1 - c_2)q \\ 0 & q(1 - c_3q + p) & (c_1 + c_2)q \\ 0 & (c_1 + c_2)q & q(1 - c_3q + p) \\ c_1 - c_2 & 0 & 0 & (1 + c_3)q^2 \end{pmatrix}, \tag{13}$$

with $q = 1 - p$. It has the eigenvalue spectrum,

$$\begin{aligned} \lambda_1^a(p) &= \frac{1}{4} + \alpha + \beta - \gamma, \lambda_2^a(p) = \frac{1}{4} - \alpha - \beta - \gamma, \\ \lambda_3^a(p) &= \frac{1}{4}(1 - \sqrt{\Delta}) + \gamma, \lambda_3^a(p) = \frac{1}{4}(1 + \sqrt{\Delta}) + \gamma, \end{aligned} \tag{14}$$

where $\alpha = \frac{c_1}{4}q, \beta = \frac{c_2}{4}q, \gamma = \frac{1}{4}(p^2 + c_3q^2)$, and $\Delta = (c_1 - c_2)^2q^2 + 4p^2$. We can obtain the entropies of the marginal states under the amplitude damping channel as $S[\text{Tr}_{A(B)}] = h(\frac{q}{2})$ for $h(x) = -x \log_2(x) - (1 - x) \log_2(1 - x)$. Obviously, the marginals of the state $\mathcal{N}_A(\rho_{AB})$ are not maximally mixed. In the followings, we will demonstrate numerically that the two-side correlations is optimal. We first consider the one-side correlations.

To calculate the one-side classical correlation in Eq. (6) of the state $\rho_{AB}^a(p)$, we take the complete set of orthonormal projectors $\{\Pi_i^B = |\Theta_i\rangle\langle\Theta_i|, i = \parallel, \perp\}$ on the subsystem B , where $|\Theta_{\parallel}\rangle = \cos(\theta)|0\rangle + \exp(i\phi) \sin(\theta)|1\rangle$ and $|\Theta_{\perp}\rangle = \exp(-i\phi) \sin(\theta)|0\rangle - \cos(\theta)|1\rangle$. The one-side classical correlation under amplitude damping channel may be written as

$$\mathcal{C}[\rho_{AB}^a(p)] = h\left(\frac{q}{2}\right) - \max(\Lambda_1, \Lambda_2, \Lambda_3), \tag{15}$$

where $\Lambda_1 = \frac{1}{2}(1 + p)h\{\frac{1}{2} + [c_3q^2 + \frac{1}{2}p(1 + p)]/(1 + p)\} + \frac{1}{2}qh(\frac{1}{2} + \frac{1}{2}|p - c_3q|)$, $\Lambda_2 = h[\frac{1}{2} + \frac{1}{2}(c_1^2q^2 + p^2)^{1/2}]$, and $\Lambda_3 = h[\frac{1}{2} + \frac{1}{2}(c_2^2q^2 + p^2)^{1/2}]$. It can be seen that the one-side classical correlation depends on the initial state ρ_{AB} and parameterized time p .

Now we consider the two-side correlations. Supposing $H(A), H(B)$ and $H(A, B)$ are the entropies of the probability distributions of the subsystem A, B and the composite system AB resulting from the complete set of projective measurement $\{\Pi_i^A \otimes \Pi_j^B, i, j = \parallel, \perp\}$ on both subsystems. Hence, we obtain

$$H(A) = H(B) = h\left\{\frac{1}{2}[1 - p \cos(2\theta)]\right\}, \tag{16}$$

$$H(A, B) = \sum_{i,j} P_{i,j}, \tag{17}$$

where $P_{\parallel,\parallel} = \frac{1}{4}\{[c_3q^2 + (1 + p)^2] \cos^4(\theta) + 2q \cos^2(\theta) \sin^2(\theta)[1 + c_1 + c_2 - c_3q + p + (c_1 - c_2) \cos(2\phi)] + (1 + c_3)q^2 \sin^4(\theta)\}$, $P_{\parallel,\perp} = P_{\perp,\parallel} = \frac{1}{4}\{q(1 - c_3q + p)(\cos^4(\theta) + \sin^4(\theta)) + \frac{1}{2}[1 - (c_1 + c_2)q + c_3q^2 + p^2 - (c_1 - c_2)q \cos(2\phi) \sin^2(2\theta)]\}$, and $P_{\perp,\perp} = \frac{1}{4}\{(1 + c_3)q^2 \cos^4(\theta) + 2q \cos^2(\theta) \sin^2(\theta)[1 + c_1 + c_2 - c_3q + p + (c_1 - c_2) \cos(2\phi)] + [c_3q^2 + (1 + p)^2] \sin^4(\theta)\}$. The two-side classical and quantum correlations are then given by

$$\mathcal{C}_t[\rho_{AB}^a(p)] = \max(\Omega_1, \Omega_2, \Omega_3), \tag{18}$$

$$\mathcal{Q}_t[\rho_{AB}^a(p)] = 2h\left(\frac{q}{2}\right) + \sum_{k=1}^4 \lambda_k \log_2 \lambda_k - \mathcal{C}_t[\rho_{AB}^a(p)], \tag{19}$$

where $\Omega_1 = \frac{1}{2}(1 + c_1q) \log_2(1 + c_1q) + \frac{1}{2}(1 - c_1q) \log_2(1 - c_1q)$, $\Omega_2 = \frac{1}{2}(1 + c_2q) \log_2(1 + c_2q) + \frac{1}{2}(1 - c_2q) \log_2(1 - c_2q)$, and $\Omega_3 = 2h(q/2) - 2 + \frac{1}{4}[c_3q^2 + (1 + p)^2] \log_2[c_3q^2 + (1 + p)^2] + \frac{1}{4}(1 + c_3)q^2 \log_2[(1 + c_3)q^2] + \frac{1}{2}q(1 - c_3q + p) \log_2[q(1 - c_3q + p)]$.

It is too tedious to compare these two types of correlations with the analytical expressions. However, we can numerically demonstrate that the two-side measures of classical correlation will not be smaller than the one-side measures for any initial state ρ_{AB} . Hence, the two-side measures of correlations are optimal for state $\rho_{AB}^a(p)$. We plot the difference of two-side and one-side measures of classical correlation dynamics $\delta = C_t[\rho_{AB}^a(p)] - C[\rho_{AB}^a(p)]$ in Fig. 1 when the initial state is a Werner state with $c_1 = -c_2 = c_3 = c(0 \leq c \leq 1)$. It can be easily seen that the difference δ is always nonnegative and becomes larger when c increasing to 1. In the followings, the investigation of the dynamics of the correlations are based on the two-side measures. It can be concluded from the expressions that we can find neither a static nor a dynamic initial state to keep the classical or quantum correlation unchanged under the amplitude damping decoherence, since the classical and quantum correlations stated in Eqs. (18) and (19) are always related with the parameterized time p . Thus, there do not exist the sudden change and sudden transition in the decay rates of the dynamics of these two correlations under amplitude damping decoherence. The dynamics of the classical and quantum correlations, the total correlation, and the entanglement which is characterized by the entanglement of formation (En) under the general condition $c_1 = 0.6, c_2 = 0.4, c_3 = -0.8$ is plotted in Fig. 2.

As proposed in Ref. [42], the Bell states $|\psi^\pm\rangle = \frac{1}{\sqrt{2}}(|01\rangle \pm |10\rangle)$ are more efficient for entanglement distribution than the Bell states $|\phi^\pm\rangle = \frac{1}{\sqrt{2}}(|00\rangle \pm |11\rangle)$ via amplitude damping channel. Here, we extend the Bell states to Werner states, and show that the quantum correlations under the amplitude damping decoherence exhibits different dynamics for different types of Werner initial states. Exactly, we first consider two types of static Werner initial states, i.e., $c_1 = -c_2 = c_3 = c$ and $c_1 = c_2 = -c_3 = c$, which correspond to $\rho_{AB}^{w_{s1}} = \frac{1-c}{4}\mathbf{I} + c|\phi^+\rangle\langle\phi^+|$ and $\rho_{AB}^{w_{s2}} = \frac{1-c}{4}\mathbf{I} + c|\psi^+\rangle\langle\psi^+|$.

Figure 3 depicts the dynamics of the classical and quantum correlations, the total correlation, and the entanglement En with $c = 0.6$. For two-qubit system, En is given by the analytical formula

$$En(\rho) = h\left[\frac{1}{2}(1 + \sqrt{1 - \gamma})\right], \tag{20}$$

where γ is the concurrence [43]. It can be seen from Fig. 3 that the quantum correlation, the total correlation and the entanglement for Werner initial state $\rho_{AB}^{w_{s2}}$ are always larger than the state $\rho_{AB}^{w_{s1}}$, while the classical correlations for the two states keep the same. Also, the entanglement sudden death exists for both Werner initial states, but state $\rho_{AB}^{w_{s2}}$ is more robust to resist this amplitude damping decoherence. It might be considered that the different dynamics of the quantum correlation for the two Werner initial states comes from the different dynamics of the entanglement. However, Fig. 4 shows that the nonentanglement quantum correlation defined as $Q_n = Q_t - En$ also

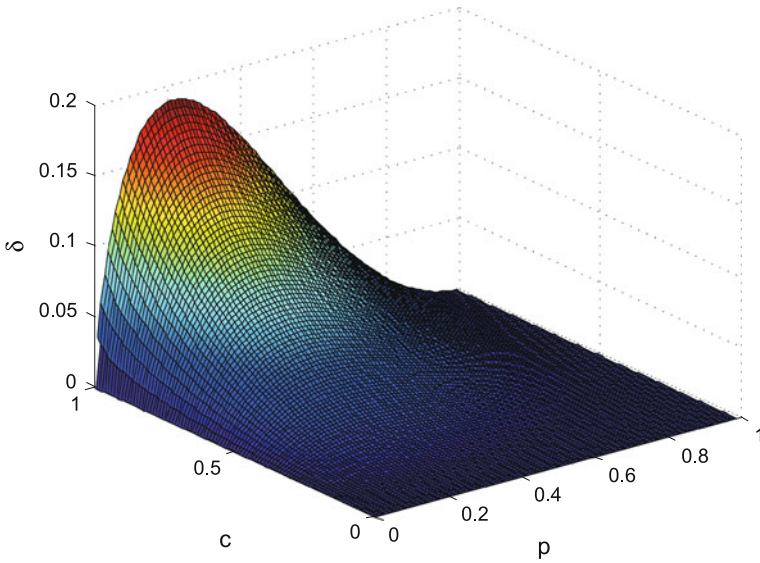


Fig. 1 The difference of two-side and one-side measures of classical correlation dynamics for amplitude damping channel with initial Werner state

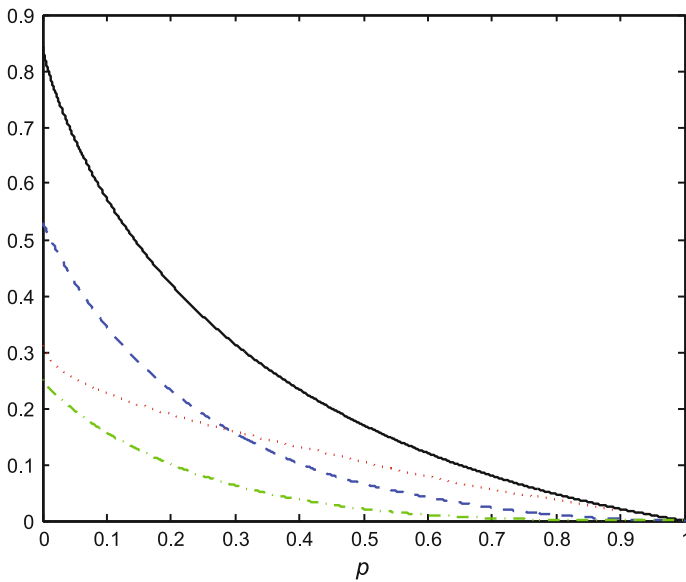


Fig. 2 The dynamics of correlations and entanglement for the two-qubit system under the amplitude damping decoherence channel for general initial states with $c_1 = 0.6$, $c_2 = 0.4$, $c_3 = -0.8$. The *solid line*, *dashed line*, *dotted line*, and *dot-dashed line* represent the total correlation, classical correlation, quantum correlation and entanglement, respectively

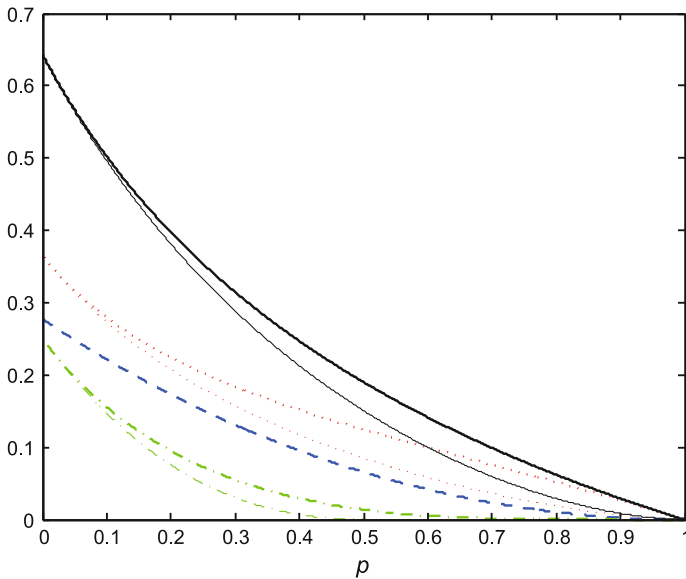


Fig. 3 The dynamics of correlations and entanglement for the two-qubit system under the amplitude damping decoherence channel for the Werner initial states with $c = 0.6$. *Thick and thin lines* denote for the static Werner initial state ρ_{AB}^{ws2} and ρ_{AB}^{ws1} . The *solid line, dashed line, dotted line, and dot-dashed line* represent the total correlation, classical correlation, quantum correlation and entanglement, respectively

contributes the difference for certain range of p , since the \mathcal{Q}_n for the two Werner initial states are not identical.

To understand the dynamics of the correlations under dissipative amplitude damping decoherence, we explore the transfers of correlations and entanglement between the two-qubit composite system and two independent environments for different types of initial states. Thus, the density operator of the initial state including the environment states is given by

$$\rho_{ABE_AE_B} = \frac{1}{4} \left(\mathbf{I}_{AB} + \sum_{i=1}^3 c_i \sigma_i^A \otimes \sigma_i^B \right) \otimes |00\rangle_{E_AE_B}, \tag{21}$$

where $|00\rangle_{E_AE_B}$ is the vacuum state of the environments E_A and E_B for subsystem A and B , respectively. Thus, the density operator of the whole output state $\mathcal{N}_a(\rho_{ABE_AE_B})$ is given by

$$\rho_{ABE_AE_B}^a(p) = \sum_{m_0, m_1} \Gamma_{m_0} \rho_{AB} \Gamma_{m_1}^\dagger \otimes |m_0\rangle_{E_AE_B} \langle m_1|_{E_AE_B}, \tag{22}$$

where $m_0, m_1 = 00, 01, 10, 11$, and $\Gamma_{ij} = (\Gamma_i^A \otimes \mathbf{I}_B)(\mathbf{I}_A \otimes \Gamma_j^B)$ for $i, j = 0, 1$. For simplicity, we only list the reduced density operators for partition E_AE_B, AE_A and AE_B (BE_B and BE_A are identical to AE_A and AE_B for symmetry) as

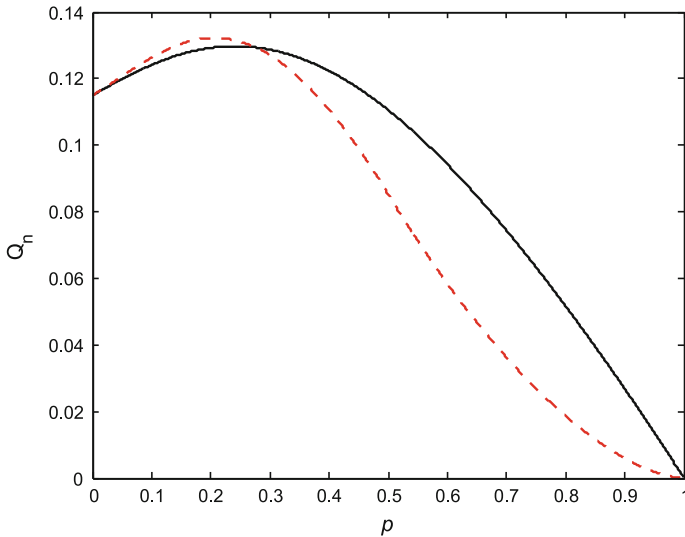


Fig. 4 The dynamics of nonentanglement quantum correlation Q_n for the two-qubit system under the amplitude damping decoherence channel for the Werner initial states with $c = 0.6$. Solid and dashed lines denote for $\rho_{AB}^{w_{s2}}$ and $\rho_{AB}^{w_{s1}}$

$$\rho_{E_A E_B}^a(p) = \frac{1}{4} \begin{pmatrix} (1+q)^2 + c_3 p^2 & 0 & (c_1 - c_2)p \\ 0 & p(2-p-c_3p) & (c_1 + c_2)p \\ 0 & (c_1 + c_2)p & p(2-p-c_3p) \\ (c_1 - c_2)p & 0 & 0 & (1+c_3)p^2 \end{pmatrix},$$

$$\rho_{A E_B}^a(p) = \frac{1}{4} \begin{pmatrix} (1+c_3)(1+pq) + 1 - c_3 & 0 & (c_1 - c_2)\sqrt{pq} \\ 0 & p(1+p-c_3q) & 0 \\ 0 & 0 & q(1+q-c_3p) & 0 \\ (c_1 - c_2)\sqrt{pq} & 0 & 0 & (1+c_3)pq \end{pmatrix},$$

and

$$\rho_{A E_A}^a(p) = \frac{1}{2} \begin{pmatrix} 1 & 0 & 0 \\ 0 & p & \sqrt{pq} \\ 0 & \sqrt{pq} & q \\ 0 & 0 & 0 \end{pmatrix}.$$

It can be seen that the dynamics of the correlations and entanglement for partition AE_A are independent of initial state, but only depend on the characteristic of amplitude damping channel. The dynamics of correlations and entanglement for partition $E_A E_B$ and AE_B are plotted in Figs. 5 and 6, when the initial states are static Werner states $\rho_{AB}^{w_{s1}}$ and $\rho_{AB}^{w_{s2}}$ with $c = 0.6$. Considering partition $E_A E_B$ in Fig. 5, the quantum and total correlation, and the entanglement for Werner initial state $\rho_{AB}^{w_{s2}}$ are always larger than the state $\rho_{AB}^{w_{s1}}$, while the classical correlations for the two states

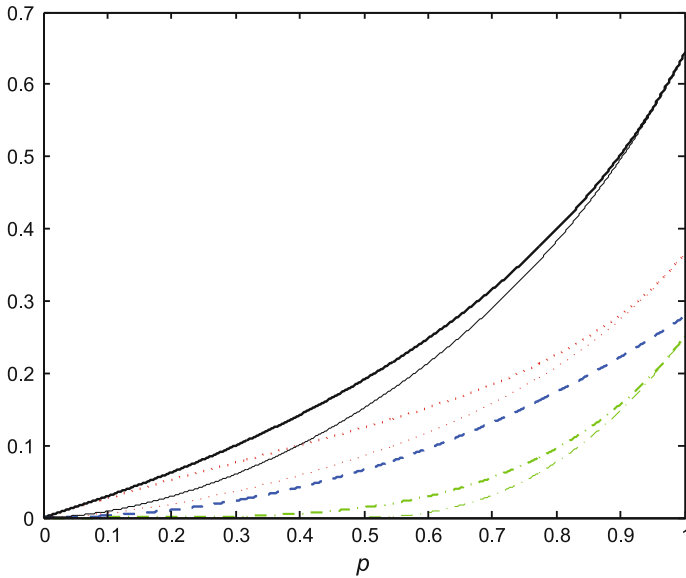


Fig. 5 The dynamics of correlations and entanglement for partition $E_A E_B$ under the amplitude damping decoherence channel for the static Werner initial state with $c = 0.6$. *Thick and thin lines* denote for the static Werner initial state $\rho_{AB}^{w_{s2}}$ and $\rho_{AB}^{w_{s1}}$ respectively. The *solid line, dashed line, dotted line, and dot-dashed line* represent the total correlation, classical correlation, quantum correlation and entanglement, respectively

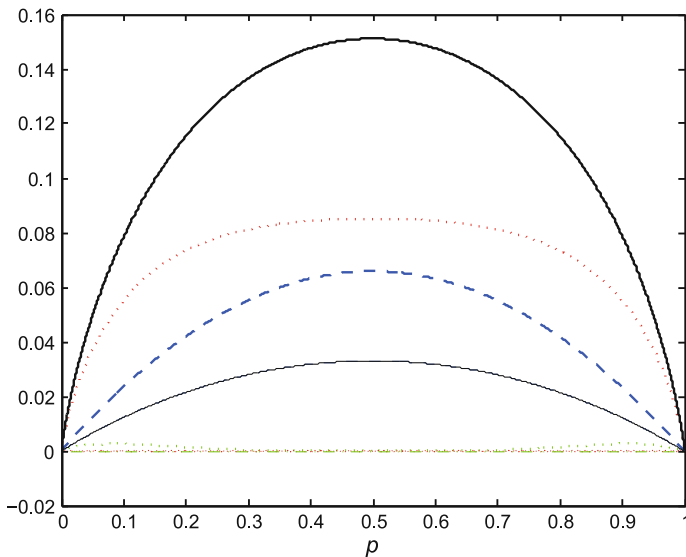


Fig. 6 The dynamics of correlations and entanglement for partition $A E_B$ under the amplitude damping decoherence channel for the static Werner initial state with $c = 0.6$. *Thick and thin lines* denote for the static Werner initial state $\rho_{AB}^{w_{s1}}$ and $\rho_{AB}^{w_{s2}}$. The *solid line, dashed line, dotted line, and dot-dashed line* represent the total correlation, classical correlation, quantum correlation and entanglement, respectively

are also identical. Thus, the correlations and entanglement for partition $E_A E_B$ is positively correlated with the correlations and entanglement of the system AB . On the contrary with the system AB , there exists a entanglement sudden birth [44] for partition $E_A E_B$ but at different p for the two static Werner initial states. However, for the partition $A E_B$, the quantum correlation and entanglement for the Werner initial state ρ_{AB}^{ws2} are both zero, and all the correlations and entanglement for Werner initial state ρ_{AB}^{ws1} are larger than state ρ_{AB}^{ws2} . Hence, the correlations and entanglement for partition $A E_B$ is negative correlated with the correlations and entanglement of the system AB .

This effect can be explained directly with the transfers of correlations and entanglement. For the Werner initial state ρ_{AB}^{ws1} under the amplitude damping decoherence, the correlations and entanglement are smaller in partition $E_A E_B$ and system AB than the initial state ρ_{AB}^{ws2} , but they are all larger in partition $A E_B$ than the initial state ρ_{AB}^{ws2} . Therefore, the correlations and entanglement are transferred more averagely to all the partitions for the Werner initial state ρ_{AB}^{ws1} , but they are more concentrated to partition $E_A E_B$ and the system AB for the Werner initial state ρ_{AB}^{ws2} .

Now we consider the case that the initial state is dynamic, i.e., the state changes with time, which includes the states with self-induced coherence or self-induced decoherence. In practice, the prepared initial quantum state may be unstable along with time, the state itself may suffer other additional influence except the considered channel decoherence. Our purpose here is to investigate the dynamic of classical and quantum correlations of the initial states which suffer other additional influence and check the infections introduced by these additional influence on the dynamic of the correlations under the decoherence channels. For simplicity, we also consider two types of dynamic Werner initial states, i.e., $c_1 = -c_2 = c_3 = p$ and $c_1 = c_2 = -c_3 = p$, which correspond to $\rho_{AB}^{wd1} = \frac{1-p}{4}I + p|\phi^+\rangle\langle\phi^+|$ and $\rho_{AB}^{wd2} = \frac{1-p}{4}I + p|\psi^+\rangle\langle\psi^+|$. These two initial states may become to the pure Bell states $|\phi^+\rangle\langle\phi^+|$ and $|\psi^+\rangle\langle\psi^+|$ with the increase of p , which is valued as the parameterized time in the quantum decoherence channel for simplicity.

The dynamics of correlations and entanglement for the two types of dynamic Werner initial states ρ_{AB}^{wd1} and ρ_{AB}^{wd2} for system AB , partition $E_A E_B$ and partition $A E_B$ are plotted in Fig. 7. It can be seen that the correlations and entanglement for dynamic Werner initial states ρ_{AB}^{wd2} are also larger than the initial state ρ_{AB}^{wd1} for system AB and partition $E_A E_B$, and smaller than the initial state ρ_{AB}^{wd1} for partition $A E_B$. These relations are the same as the case of the static Werner initial state ρ_{AB}^{ws1} and ρ_{AB}^{ws2} . As p increasing to 1, the correlations and entanglement for partition $A E_B$ and partition $E_A E_B$ are also the similar as the static Werner initial state. However, the correlations and entanglement vanish asymptotically for the system AB . And interestingly, we find entanglement sudden birth for all the partitions. This is because, on the one hand, the increase of p increases the entanglement of the initial states, but on the other hand, it enhances the channel decoherence. The system-reservoir dynamics of classical and quantum correlations under the amplitude damping decoherence channel have also been studied in Ref. [29]. However, this work focuses on the consideration of one kind of static Werner initial state, the dynamic Werner initial states and comparative study of different kinds of Werner initial states are out of consideration.

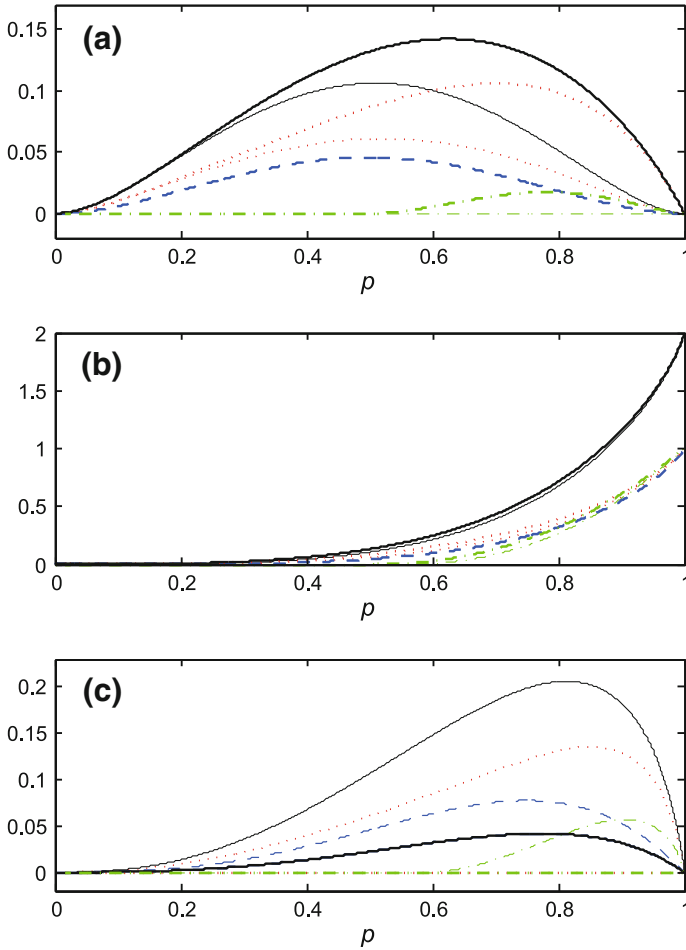


Fig. 7 The dynamics of correlations and entanglement for **a** system AB , **b** partition $E_A E_B$ and **c** partition $A E_B$ under the amplitude damping decoherence channel for dynamic Werner initial states. *Thick and thin lines* denote for the dynamic Werner initial state ρ_{AB}^{wd2} and ρ_{AB}^{wd1} . The *solid line, dashed line, dotted line, and dot-dashed line* represent the total correlation, classical correlation, quantum correlation and entanglement, respectively

3.2 Depolarizing channel

The depolarizing channel \mathcal{N}_D is a nondissipative channel with Kraus operators,

$$\Gamma_0^k = \sqrt{1 - \frac{3pk}{4}} \mathbf{I}, \Gamma_i^k = \frac{\sqrt{pk}}{2} \sigma_i (i = 1, 2, 3), \tag{23}$$

for $k = A, B$. We also consider the symmetric situation here, i.e., $p_A = p_B \equiv p$. The density operator of the state $\mathcal{N}_D(\rho_{AB})$ under the multimode depolarizing channel may be written as

$$\rho_{AB}^d(p) = \frac{1}{4} \begin{pmatrix} 1 + c_3q^2 & 0 & 0 & (c_1 - c_2)q^2 \\ 0 & 1 - c_3q^2 & (c_1 + c_2)q^2 & 0 \\ 0 & (c_1 + c_2)q^2 & 1 - c_3q^2 & 0 \\ (c_1 - c_2)q^2 & 0 & 0 & 1 + c_3q^2 \end{pmatrix}, \quad (24)$$

which has the eigenvalue spectrum,

$$\begin{aligned} \lambda_1^d(p) &= \frac{1}{4}[1 + (c_1 - c_2 + c_3)q^2], \lambda_2^d(p) = \frac{1}{4}[1 - (c_1 - c_2 - c_3)q^2], \\ \lambda_3^d(p) &= \frac{1}{4}[1 + (c_1 + c_2 - c_3)q^2], \lambda_4^d(p) = \frac{1}{4}[1 - (c_1 + c_2 + c_3)q^2]. \end{aligned} \quad (25)$$

Thus, the state $\mathcal{N}_D(\rho_{AB})$ can be also written as

$$\begin{aligned} \rho_{AB}^d(p) &= \lambda_1^d(p)|\phi^+\rangle\langle\phi^+| + \lambda_2^d(p)|\phi^-\rangle\langle\phi^-| + \lambda_3^d(p)|\psi^+\rangle\langle\psi^+| \\ &\quad + \lambda_4^d(p)|\psi^-\rangle\langle\psi^-|. \end{aligned} \quad (26)$$

The entropies of the marginal states remain constant under the depolarizing channel, i.e., $S[\text{Tr}_{A(B)}\rho_{AB}^d(p)] = 1$. We take the complete set of orthonormal projectors $\{\Pi_i^B = |\Theta_i\rangle\langle\Theta_i|, i = \parallel, \perp\}$ on the subsystem B . Then the reduced measured density operator of the subsystem A under the depolarizing channel, $\rho_A^i = \text{Tr}_B[\Pi_i^B \mathcal{N}_D(\rho_{AB}) \Pi_i^B]/q_i$, has the following eigenvalue spectrum,

$$\begin{aligned} \xi_{1,2}^i &= \frac{1}{2} \pm \frac{1}{4}q^2[c_1^2 + c_2^2 + 2c_3^2 - (c_1^2 + c_2^2 - 2c_3^2) \cos(4\theta) \\ &\quad + 2(c_1 + c_2) \cos(2\phi) \sin^2(2\theta)], \end{aligned} \quad (27)$$

and $q_i = \frac{1}{2}$ for $i = \parallel, \perp$. Hence, the one-side measures of classical correlation is identical to the two-side measures of classical correlation. The classical and quantum correlations under the depolarizing decoherence are given by

$$\mathcal{C}[\rho_{AB}^d(p)] = 1 + h \left[\frac{1}{2}(1 - \chi) \right], \quad (28)$$

$$\mathcal{D}[\rho_{AB}^d(p)] = 2 + \sum_{k=1}^4 \lambda_k^d(p) \log_2 \lambda_k^d(p) - \mathcal{C}[\rho_{AB}^d(p)], \quad (29)$$

where $\chi = \max(c_1q^2, c_2q^2, c_3q^2)$.

On the other hand, the quantum discord can be measured as relative entropy to its closest classical state [19]. The closest classical state of the Bell-diagonal state $\rho_{AB}^d(p)$ in Eq. (26) is given by

$$\rho_{cl} = \frac{\kappa(p)}{2} \sum_{i=1,2} |\Psi_i\rangle\langle\Psi_i| + \frac{1 - \kappa(p)}{2} \sum_{i=3,4} |\Psi_i\rangle\langle\Psi_i|, \quad (30)$$

with $\kappa(p) = \lambda_1^d(p) + \lambda_2^d(p)$, where $\lambda_1^d(p)$, $\lambda_2^d(p)$ are the two largest eigenvalues given by Eq. (25), and $|\Psi_i\rangle$ are the corresponding Bell states. From Eq. (25), for a fixed initial state, the two largest eigenvalues will be independent of p . Then the quantum discord, i.e., the distance from the state $\rho_{AB}^d(p)$ to its closest classical state ρ_{cl} will not change for any p . Therefore, there do not exist sudden change and sudden transition in the decay rates of both the classical and quantum correlations for any initial state under the action of depolarizing decoherence, this is different from the other kinds of non-dissipative channels, i.e. bit flip, phase flip and bit-phase flip decoherence channels. The dynamics of the classical and quantum correlations, the total correlation, and the entanglement En under the general condition $c_1 = 0.6, c_2 = 0.4, c_3 = -0.8$ is plotted in Fig. 8.

Considering the static Werner states ρ_{AB}^{ws1} and ρ_{AB}^{ws2} as the initial states, the dynamics of the correlations and entanglement for these two initial states are identical. Also, we find the dynamics of the correlations and entanglement for the dynamic Werner initial states ρ_{AB}^{wd1} and ρ_{AB}^{wd2} are identical. The dynamics of the correlations and entanglement for ρ_{AB}^{ws1} with $c = 0.6$ and ρ_{AB}^{wd1} are plotted in Figs. 9 and 10. For the other nondissipative channels, such as the bit flip, phase flip and bit-phase flip decoherence channels, the correlations of the two different types of Werner states can be found also exhibit the same dynamics from [28].

Interestingly, the dynamics of the quantum dissonance Q_d under the depolarizing decoherence for static Werner initial states ρ_{AB}^{ws1} and ρ_{AB}^{ws2} are an identical constant value, which is obtained as $Q_d = 0.1258$ with independent of the value of c and p .

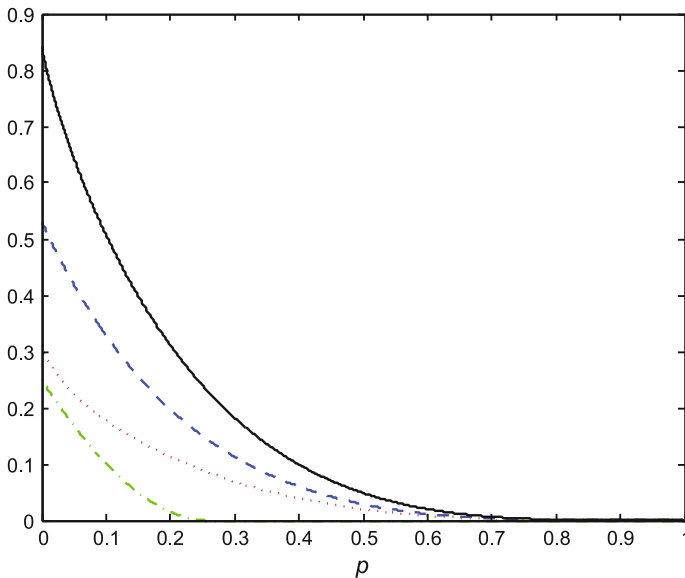


Fig. 8 The dynamics of correlations and entanglement under the depolarizing decoherence channel for general initial states with $c_1 = 0.6, c_2 = 0.4, c_3 = -0.8$. The *solid line*, *dashed line*, *dotted line*, and *dot-dashed line* represent the total correlation, classical correlation, quantum correlation and entanglement, respectively

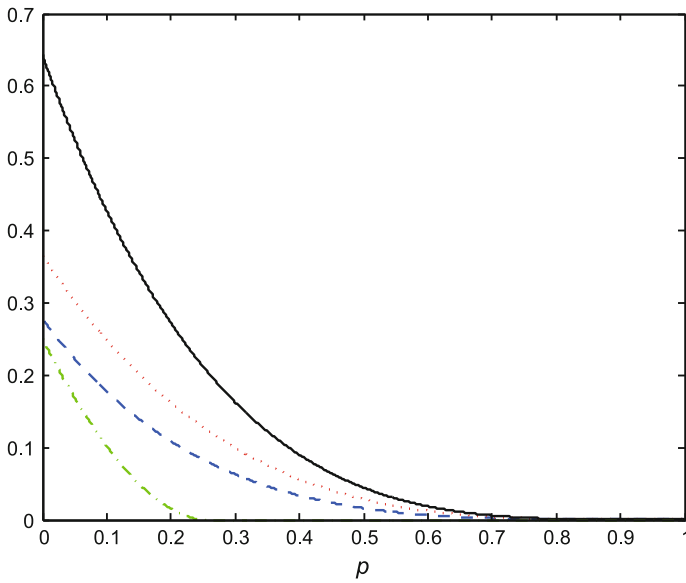


Fig. 9 The dynamics of correlations and entanglement under the depolarizing decoherence channel for the static Werner initial state ρ_{AB}^{ws1} with $c = 0.6$. The *solid line*, *dashed line*, *dotted line*, and *dot-dashed line* represent the total correlation, classical correlation, quantum correlation and entanglement, respectively

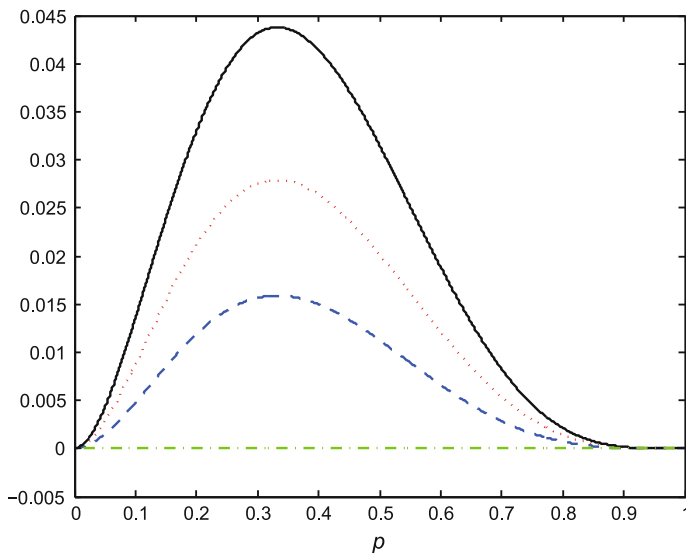


Fig. 10 The dynamics of correlations and entanglement under the depolarizing decoherence channel for the dynamic Werner initial state ρ_{AB}^{wd1} . The *solid line*, *dashed line*, *dotted line*, and *dot-dashed line* represent the total correlation, classical correlation, quantum correlation and entanglement, respectively

This is because the closest separable state of the ρ_{AB}^d and its closest classical state are determined under this situation. However, the quantum dissonance of the unentangled states ρ_{AB}^u with $c_1 = c_2 = 0, c_3 = c$ will increase monotonically to the fixed value, since $\rho_{AB}^d(p = 1) = \frac{1}{4}I$. The dynamics of quantum dissonance Q_d and entanglement for the Werner initial states ρ_{AB}^{ws1} and unentangled state ρ_{AB}^u with $c = 0.6$ are depicted in Fig. 11. By comparison to the dynamic of the quantum correlation for the Werner initial state ρ_{AB}^{ws1} in Fig. 9, we can conclude that the constant quantum dissonance Q_d in this situation do not give a contribution on the decay of the quantum correlation (quantum discord). However, this coincides with the subadditivity of correlations, since the quantum dissonance and entanglement do not add to give the quantum discord but larger than it [19].

Thus, we show there exist differences of the dynamics of classical and quantum correlations under the nondissipative and dissipative decoherence channels, since the dynamics of correlations and entanglement are different under the dissipative decoherence channels and identical under the nondissipative decoherence channels for different types of initial states. And also, the dynamics of correlations are different under different nondissipative decoherence channels. These differences of dynamics come from the different types of interaction to the environments. For the dissipative channels, there exist exchanges of energy between the system and the environment. The outcomes show that the exchange of energy for amplitude channel suggests different dynamics of correlations and entanglement for different kinds of initial states. While for the nondissipative channels, the exchanges of energy do not exist.

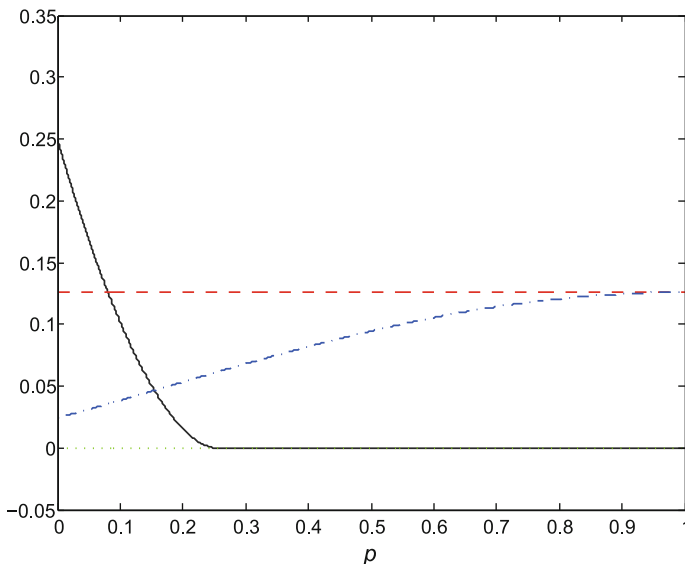


Fig. 11 The dynamics of quantum dissonance Q_d and entanglement for the Werner initial states ρ_{AB}^{ws1} and unentangled state ρ_{AB}^u with $c = 0.6$. The solid line, dashed line, dotted line, and dot-dashed line represent the entanglement for ρ_{AB}^{ws1} , quantum dissonance for ρ_{AB}^{ws1} , entanglement for ρ_{AB}^u and quantum dissonance for ρ_{AB}^u , respectively

4 Conclusion

We investigate the dynamics of classical and quantum correlations under nondissipative and dissipative decoherences with analytically and numerically methods based on one-side measures and two-side measures. Exactly, we investigate two qubits under local depolarizing decoherence channel and amplitude damping decoherence channel for the static and dynamic initial states. We show that, under the action of amplitude damping decoherence, for two types of static and dynamic Werner initial states with the same initial entanglement and correlations, exhibit different types of dynamics. Specifically, the type of Werner states $\rho_{AB}^{ws2}, \rho_{AB}^{wd2}$ are more robust to resist decoherence than the states $\rho_{AB}^{ws1}, \rho_{AB}^{wd1}$ correspondingly. Moreover, the transfers of the entanglement and correlations between the system and the independent environments are explored. It can be seen that the transfers of the correlations and entanglement for the type of Werner states ρ_{AB}^{ws1} are more average to different partitions than the states ρ_{AB}^{ws2} .

While for the action of depolarizing decoherence, we show numerically that there does not exist sudden change in the decay rates of both the classical and quantum correlations, and the classical and quantum correlations can not keep unchanged under the decoherence, which is different from some other nondissipative channels, such as the phase flip, bit flip and bit-phase flip decoherence channels. It has demonstrated that the classical and quantum correlations can keep unchanged and there exist sudden change and sudden transition under these decoherence channels. Also, the dynamics of the correlations and entanglement for the two types of static and dynamic Werner initial states are found to be identical. Furthermore, the quantum dissonance for the static Werner initial state ρ_{AB}^{ws1} and ρ_{AB}^{ws2} can be unaffected, but the quantum dissonance of the unentangled states increases monotonically by the action of depolarizing decoherence. Such different dynamic behaviors of different noisy quantum decoherence channels reveal distinct transmission performance of classical and quantum information. This performance of the correlations and entanglement for different types of quantum states are useful for quantum communication and quantum computation.

Acknowledgments This work was supported by the National Natural Science Foundation of China (Grant No. 60773085, No. 60970109, and No. 60801051), and NSFC-KOSEF International Collaborative Research Funds (Grant No. 60811140346, and No. F01-2008-000-10021-0).

Appendix

Calculation of the quantum dissonance Q_d of the Bell-diagonal states. Consider the Bell-diagonal state $\rho = \sum_{i=1}^4 \lambda_i |\Psi_i\rangle\langle\Psi_i|$, where λ_i are ordered in nonincreasing size and $|\Psi_i\rangle$ are the four Bell states. The closest separable state is $\sigma = \sum_{i=1}^4 p_i |\Psi_i\rangle\langle\Psi_i|$ where $p_1 = 1/2$ and the other probabilities are $p_i = \lambda_i/[2(1 - \lambda_1)]$ [39]. Also, the closest classical state for σ is obtained as $\chi = \sum_{i=1}^4 q_i |\Psi_i\rangle\langle\Psi_i|$, where $q_{1,2} = (p_1 + p_2)/2, q_{3,4} = (1 - p_1 - p_2)/2$. The quantum dissonance of state ρ can be calculated as

$$Q_d = S(\sigma \parallel \chi)$$

$$\begin{aligned}
 &= -\text{Tr}(\sigma \log_2 \chi) + \text{Tr}(\sigma \log_2 \sigma) \\
 &= -\text{Tr} \left(\sum_{i=1}^4 p_i |\Psi_i\rangle \langle \Psi_i| \log_2 \sum_{i=1}^4 q_i |\Psi_i\rangle \langle \Psi_i| \right) \\
 &\quad + \text{Tr} \left(\sum_{i=1}^4 p_i |\Psi_i\rangle \langle \Psi_i| \log_2 \sum_{i=1}^4 p_i |\Psi_i\rangle \langle \Psi_i| \right) \\
 &= -\sum_{i=1}^4 p_i \log_2 q_i + \sum_{i=1}^4 p_i \log_2 p_i \\
 &= 1 + \sum_{i=1}^4 p_i \log_2 p_i - (p_1 + p_2) \log_2 (p_1 + p_2) \\
 &\quad - (1 - p_1 - p_2) \log_2 (1 - p_1 - p_2). \tag{31}
 \end{aligned}$$

References

1. Einstein, A., Podolsky, B., Rosen, N.: Can quantum-mechanical description of physical reality be considered complete? *Phys. Rev.* **47**(10), 777–780 (1935)
2. Horodecki, R., Horodecki, P., Horodecki, M., Horodecki, K.: Quantum entanglement. *Rev. Mod. Phys.* **81**(2), 865–942 (2009)
3. Yu, T., Eberly, J.H.: Quantum open system theory: bipartite aspects. *Phys. Rev. Lett.* **97**(14), 140403 (2006)
4. Xu, J.S., Li, C.F., Gong, M., Zou, X.B., Shi, C.H. et al.: Experimental demonstration of photonic entanglement collapse and revival. *Phys. Rev. Lett.* **104**(10), 100502 (2010)
5. Meyer, D.A.: Sophisticated quantum search without entanglement. *Phys. Rev. Lett.* **85**(9), 2014–2017 (2000)
6. Kenigsberg, D., Mor, T., Ratsaby, G.: Quantum advantage without entanglement. *Quantum Inf. Comput.* **6**(7), 606–615 (2006)
7. Datta, A., Shaji, A., Caves, C.M.: Quantum discord and the power of one qubit. *Phys. Rev. Lett.* **100**(5), 050502 (2008)
8. Lanyon, B.P., Barbieri, M., Almeida, M.P., White, A.G.: Experimental quantum computing without entanglement. *Phys. Rev. Lett.* **101**(20), 200501 (2008)
9. Henderson, L., Vedral, V.: Classical, quantum and total correlations. *J. Phys. A Math. Gen.* **34**(35), 6899–6905 (2001)
10. Ollivier, H., Zurek, W.H.: Quantum discord: a measure of the quantumness of correlations. *Phys. Rev. Lett.* **88**(1), 017901 (2001)
11. Werner, R.F.: Quantum states with Einstein-Podolsky-Rosen correlations admitting a hidden-variable model. *Phys. Rev. A* **40**(8), 4277–4281 (1989)
12. Ollivier, H., Zurek, W.H.: Quantum discord: a measure of the quantumness of correlations. *Phys. Rev. Lett.* **88**(1), 017901 (2001)
13. Oppenheim, J., Horodecki, M., Horodecki, P., Horodecki, R.: Thermodynamical approach to quantifying quantum correlations. *Phys. Rev. Lett.* **89**(18), 180402 (2002)
14. Terhal, B.M., Horodecki, M., Leung, D.W., DiVincenzo, D.P.: The entanglement of purification. *J. Math. Phys.* **43**(9), 4286–4298 (2002)
15. DiVincenzo, D.P., Horodecki, M., Leung, D.W., Smolin, J.A., Terhal, B.M.: Locking classical correlations in quantum states. *Phys. Rev. Lett.* **92**(6), 067902 (2004)
16. Horodecki, M., Horodecki, P., Horodecki, R., Oppenheim, J. et al.: Local versus nonlocal information in quantum-information theory: formalism and phenomena. *Phys. Rev. A* **71**(6), 062307 (2005)
17. Groisman, B., Popescu, S., Winter, A.: Quantum, classical, and total amount of correlations in a quantum state. *Phys. Rev. A* **72**(3), 032317 (2005)

18. Luo, S.: Using measurement-induced disturbance to characterize correlations as classical or quantum. *Phys. Rev. A* **77**(2), 022301 (2008)
19. Modi, K., Paterek, T., Son, W., Vedral, V., Williamson, M.: Unified view of quantum and classical correlations. *Phys. Rev. Lett.* **104**(8), 080501 (2010)
20. Zurek, W.H.: Quantum discord and Maxwells demons. *Phys. Rev. A* **67**(1), 012320 (2003)
21. Rodriguez-Rosario, C.A., Modi, K., Kuah, A.M., Shaji, A., Sudarshan, E.C.G.: Completely positive maps and classical correlations. *J. Phys. A Math. Theor.* **41**(20), 205301 (2008)
22. Piani, M., Horodecki, P., Horodecki, R.: No-local-broadcasting theorem for multipartite quantum correlations. *Phys. Rev. Lett.* **100**(9), 090502 (2008)
23. Luo, S.: Quantum discord for two-qubit systems. *Phys. Rev. A* **77**(4), 042303 (2008)
24. Werlang, T., Souza, S., Fanchini, F.F., Boas, C.J.V.: Robustness of quantum discord to sudden death. *Phys. Rev. A* **80**(2), 024103 (2009)
25. Ferraro, A., Aolita, L., Cavalcanti, D., Cucchietti, F.M., Acin, A.: Almost all quantum states have nonclassical correlations. *Phys. Rev. A* **81**(5), 052318 (2010)
26. Wang, B., Xu, Z.Y., Chen, Z.Q., Feng, M.: Non-Markovian effect on the quantum discord. *Phys. Rev. A* **81**(1), 014101 (2010)
27. Fanchini, F.F., Werlang, T., Brasil, C.A., Arruda, L.G.E., Caldeira, A.O.: Non-Markovian dynamics of quantum discord. *Phys. Rev. A* **81**(5), 052107 (2010)
28. Maziero, J., Céleri, C.L., Serra, R.M., Vedral, V.: Classical and quantum correlations under decoherence. *Phys. Rev. A* **80**(4), 044102 (2009)
29. Maziero, J., Werlang, T., Fanchini, F.F., Céleri, C.L., Serra, R.M.: System-reservoir dynamics of quantum and classical correlations. *Phys. Rev. A* **81**(2), 022116 (2010)
30. Sarandy, M.S.: Classical correlation and quantum discord in critical systems. *Phys. Rev. A* **80**(2), 022108 (2009)
31. Luo, S., Zhang, Q.: Observable Correlations in two-qubit states. *J. Stat. Phys.* **136**(1), 165–177 (2009)
32. Xu, J.S., Xu, X.Y., Li, C.F., Zhang, C.J. et al.: Experimental investigation of classical and quantum correlations under decoherence. *Nat. Commun.* **1**, 7 (2010)
33. Berrada, K., Eleuch, H., Hassouni, Y.: Asymptotic dynamics of quantum discord in open quantum systems. *J. Phys. B At. Mol. Opt. Phys.* **44**(14), 145503 (2011)
34. Schumacher, B., Westmoreland, M.D.: Quantum mutual information and the one-time pad. *Phys. Rev. A* **74**(4), 042305 (2006)
35. Vedral, V.: The elusive source of quantum effectiveness. <http://arxiv.org/abs/0906.3656> (2009)
36. Mazzola, L., Piilo, J., Maniscalco, S.: Sudden transition between classical and quantum decoherence. *Phys. Rev. Lett.* **104**(20), 200401 (2010)
37. Cover, T.M., Thomas, J.A.: *Elements of Information Theory*. Wiley, New York (2006)
38. Vedral, V., Plenio, M.B., Rippin, M.A., Knight, P.L.: Quantifying entanglement. *Phys. Rev. Lett.* **78**(12), 2275–2279 (1997)
39. Vedral, V., Plenio, M.B.: Entanglement measures and purification procedures. *Phys. Rev. A* **57**(3), 1619–1633 (1998)
40. Kraus, K.: *States, Effects, and Operations: Fundamental Notions of Quantum Theory*. Springer, Berlin (1983)
41. Nielsen, M.A., Chuang, I.L.: *Quantum Computation and Quantum Information*. Cambridge University Press, Cambridge, UK (2000)
42. Wang, Q., Tan, M.Y., Liu, Y., Zeng, H.S.: Entanglement distribution via noisy quantum channels. *J. Phys. B At. Mol. Opt. Phys.* **42**(12), 125503 (2009)
43. Wootters, W.K.: Entanglement of formation of an arbitrary state of two qubits. *Phys. Rev. Lett.* **80**(10), 2245–2248 (1998)
44. López, C.E., Romero, G., Lastra, F. et al.: Sudden birth versus sudden death of entanglement in multipartite systems. *Phys. Rev. Lett.* **101**(8), 080503 (2008)